

# A Simple Baryon Triality Model for Neutrino Masses

Herbi K. Dreiner,<sup>\*</sup> Jong Soo Kim,<sup>†</sup> and Marc Thormeier<sup>‡</sup>

*Physikalisches Institut der Universität Bonn  
Nußallee 12, 53115 Bonn, Germany*

(Dated: February 2, 2008)

We make a simple ansatz for the supersymmetric lepton-number violating Yukawa couplings, by relating them to the corresponding Higgs Yukawa couplings. This reduces the free  $B_3$  parameters from 36 to 6. We fit these parameters to solve the solar and atmospheric neutrino anomalies in terms of neutrino oscillations. The resulting couplings are consistent with the stringent low-energy bounds. We investigate the resulting LHC collider signals for a stau LSP scenario.

## I. INTRODUCTION

The first experimental evidence for physics beyond the Standard Model (SM) has been found in the neutrino sector [1]. The solar and atmospheric neutrino anomalies are best explained in terms of oscillating massive neutrinos [2], as opposed to for example lepton flavour-violating interactions [3]. Assuming massive neutrinos, based on a three neutrino fit including the recent MINOS [4] and the SK-II atmospheric data [5], the corresponding neutrino mass and mixing parameters at  $1\sigma$  ( $3\sigma$ ) C.L. are [6, 7]

$$\Delta m_{21}^2 = 7.9^{+0.27}_{-0.28} \left( \begin{smallmatrix} +1.1 \\ -0.89 \end{smallmatrix} \right) \times 10^{-5} \text{eV}^2, \quad (1)$$

$$|\Delta m_{31}^2| = 2.6 \pm 0.2 (0.6) \times 10^{-3} \text{eV}^2, \quad (2)$$

$$\theta_{12} = 33.7 \pm 1.3 \left( \begin{smallmatrix} +4.3 \\ -3.5 \end{smallmatrix} \right), \quad (3)$$

$$\theta_{23} = 43.3^{+4.3}_{-3.8} \left( \begin{smallmatrix} +9.8 \\ -8.8 \end{smallmatrix} \right), \quad (4)$$

$$\theta_{13} = 0^{+5.2}_{-0.0} \left( \begin{smallmatrix} +11.5 \\ -0.0 \end{smallmatrix} \right). \quad (5)$$

The angles are given in degrees. The most widely discussed extensions of the SM to include massive neutrinos involve the see-saw mechanism [8]. These require right-handed neutrinos, as well as a new, typically very large Majorana mass-scale. The see-saw mechanism can also be incorporated into the minimal supersymmetric SM (MSSM) [9], now requiring right-handed neutrino superfields, as well as the additional high mass scale.

However, within supersymmetry there is another, in our opinion simpler, possibility to include massive neutrinos, namely via *renormalizable* lepton-number violating terms,  $W_{\mathcal{L}_i}$ , in the superpotential [10],

$$W_{\mathcal{L}_i} = \lambda_{ijk} L_i L_j \bar{E}_k + \lambda'_{ijk} L_i Q_j \bar{D}_k + \kappa_i L_i H_u, \quad (6)$$

$$W_{H_d} = h_{ij}^E L_i H_d \bar{E}_j + h_{ij}^D Q_i H_d \bar{D}_j + \mu H_d H_u, \quad (7)$$

where we have employed the conventional notation for the superfields [11]. For later use, we have also included the superpotential terms involving the down-like Higgs superfield. The terms in  $W_{\mathcal{L}_i}$  violate  $R$ -parity (a  $\mathbb{Z}_2$ -symmetry) as well as proton hexality [12, 13] (a  $\mathbb{Z}_6$ -symmetry), but conserve baryon triality ( $B_3$ , a  $\mathbb{Z}_3$ -symmetry, sometimes also misleadingly called baryon parity) [14, 15, 16]. The Majorana neutrino masses are generated via tree-level mixing with the neutralinos, as well as via radiative corrections [10, 17, 18, 19, 20, 21, 22]. There is an implicit see-saw mechanism in the neutralino-neutrino sector:  $\kappa_i^2/M_{1/2}$ , but with a much smaller hierarchy of mass scales. Furthermore, no new fields or mass scales are required.

Within a baryon triality supergravity model the largest neutrino mass is naturally small [11]. For universal soft breaking terms, the mixing,  $\kappa_i$ , with the neutralinos is zero at the unification scale. It is subsequently generated at the order of a few MeV via renormalization group equations. It is thus proportional to the product of a (small) down-like Higgs Yukawa coupling (for example of the bottom quark or the tau lepton), a (small) baryon triality coupling and the Higgs mixing parameter  $\mu$  [11, 23, 24, 25]. The lighter neutrino masses are generated via radiative corrections, and are naturally further suppressed.

There are  $9 + 27 + 3 = 39$  lepton-number violating (complex) parameters in the superpotential  $W_{\mathcal{L}}$ . There are also 39 corresponding soft-supersymmetry breaking parameters, which in principle are independent, but are usually related to those of  $W_{\mathcal{L}}$  via universal soft-supersymmetry breaking [26]. In a top-down approach, *e.g.* based on the Froggatt-Nielsen mechanism [27], one can attempt to predict the order of magnitude of all superpotential parameters, *i.e.*  $W_{\mathcal{L}_p}$  together with the Higgs Yukawa couplings, based on a spontaneously broken gauge symmetry, Ref. [28, 29] and references therein. See also Refs. [21, 22, 30, 31].

In this letter, we instead propose a baryon tri-

<sup>\*</sup>E-mail: dreiner@th.physik.uni-bonn.de

<sup>†</sup>E-mail: jsk@th.physik.uni-bonn.de

<sup>‡</sup>E-mail: thor@th.physik.uni-bonn.de

ality model of neutrino masses, based on a simple phenomenological ansatz, which relates the Higgs superpotential parameters to those that violate lepton-number. The justification for this is that the down-like Higgs doublet superfield and the lepton-doublet superfields have identical Standard Model gauge quantum numbers. We make no assumption about the possible underlying theory at the unification scale. This ansatz dramatically reduces the number of free parameters. If experimentally confirmed it would give a clear indication on how to construct the more fundamental unified theory.

In the literature there are other simple ansätze [32, 33, 34], the most common and also the most similar to ours is pure bi-linear lepton-number violation, *i.e.*  $\lambda_{ijk} = \lambda'_{ijk} = 0$ , and  $\kappa_i \neq 0$ . For this there is an extensive literature, see for example [17, 18, 21, 30, 35, 36] and references therein. We discuss how our ansatz differs from the bi-linear case in Sect. III.

A special feature of baryon triality models for the neutrino masses, is that they lead to other observable effects at colliders and can thus be tested [34, 37, 38, 39, 40, 41, 42, 43, 44, 45, 46, 47, 48, 49, 50, 51, 52]. In the case of pure tri-linear couplings ( $\kappa_i = 0$ ), a fit to the neutrino data, Eqs. (1)-(5), leads to values in the range  $\lambda_{ijk}, \lambda'_{ijk} \sim 10^{-5} - 10^{-4}$  [53, 54, 55, 56]. These couplings are very small, in particular, too small for the resonant production of supersymmetric particles [57]. However, they do lead to the decay of the lightest supersymmetric particle in the detector, possibly with a detached vertex. This model can be confirmed by measuring the branching ratios of the various lightest supersymmetric particle (LSP) decays and thereby measuring the couplings. However, several points have in my opinion been missed in the literature. In the case of a pure fit, *i.e.* not a model, it is possible to have larger couplings, which do not contribute to the neutrino masses, or which are not required for the fit. In this case, the LSP decay which dominates the collider signals will be completely independent of the neutrino sector. Thus pure fit models can only be tested if the neutrino mass parameters dominate the  $B_3$  sector. We consider here a complete model, where the fit to the neutrino data fixes *all* the  $B_3$  parameters. Second, it has hitherto been assumed, that the LSP is the lightest neutralino. We go beyond this and also consider a scalar tau LSP [11, 58].

Our analysis is structured as follows: In Sect. II, we present our model in detail. We then briefly review the neutrino masses in baryon triality models, Sect. IV. In Sect. V, we estimate the values of the free parameters which result in acceptable neutrino masses. In Sect. VI, we numerically evaluate the new parameters in our model, such that the neutrino masses and mixing angles fall in the required experimental ranges, *cf* Eqs. (1)-(5). In order to obtain at least two non-vanishing neutrino masses, we must violate

at least two lepton numbers. This typically leads to significantly stricter bounds on the products of couplings [59, 60, 61, 62]. In Sect. VII, we investigate, whether our model is consistent with these bounds. In Sect. VIII, we discuss possible future tests of the ansatz at colliders, in particular the LHC. In Sect. IX we conclude.

## II. SIMPLE $B_3$ -MODEL

In the MSSM, the lepton doublet superfields  $L_i$  and the down-type Higgs superfield  $H_d$  have the same gauge quantum numbers. They are distinguished through a discrete symmetry: lepton number. However, in the case of baryon triality, lepton number is violated and not well defined. In the most general baryon triality superpotential with the MSSM superfields,  $H_d$  and  $L_i$  have exactly corresponding terms in the superpotential, as can be seen in Eqs. (6) and (7). We take this correspondence to motivate the following simple ansatz for the Yukawa coupling constants

$$\lambda_{ijk} \equiv \ell_i \cdot h_{jk}^E - \ell_j \cdot h_{ik}^E, \quad (8)$$

$$\lambda'_{ijk} \equiv \ell'_i \cdot h_{jk}^D, \quad (9)$$

$$\kappa_i \equiv c_i \cdot \mu. \quad (10)$$

Here,  $\ell_i, \ell'_i$  are *c*-numbers. Eq. (8) has the required form to maintain the anti-symmetry of the  $\lambda_{ijk}$  in the first two indices. The ansatz for the dimensionful mixing terms, Eq. (10), is no simplification and we retain the  $\kappa_i$  as free parameters. Given the ansatz of Eqs. (8), (9), and assuming we know the Higgs-Yukawa coupling constants (leading to the SM fermion mass matrices), then the 36 couplings  $\lambda_{ijk}, \lambda'_{ijk}$ , are parameterized in terms of the six numbers  $\ell_i, \ell'_j$ .

Since  $L_i$  and  $H_d$  have the same *gauge* quantum numbers, our ansatz in Eqs. (8),(9) is given in the  $SU(2) \times U(1)$  *current*-eigenstate basis. Thus when computing neutrino masses and comparing the required Yukawa coupling constants to low-energy bounds, we must rotate to the mass-eigenstate basis [63, 64]. This requires a bi-unitary transformation in generation space. We shall denote the transformation of the left-handed and right-handed fermions (not superfields), respectively by

$$e_L = V_e e'_L, \quad d_L = V_d d'_L, \quad u_L = V_u u'_L, \quad (11)$$

$$e_R = U_e e'_R, \quad d_R = U_d d'_R, \quad u_R = U_u u'_R, \quad (12)$$

where  $V_{e,d,u}, U_{e,d,u}$  are  $3 \times 3$  matrices in generation space and the prime denotes the mass-eigenstates. We have combined the charged lepton and quark states into three-component vectors in generation space, *e.g.*  $e_L \equiv (e_L, \mu_L, \tau_L)$ . We rotate the sfermion partners by the same matrices in flavour space. By construction, these transformations diagonalize the SM

Coupling	Model Value	Numerical Value ( $\tan \beta = 10$ )
$\lambda_{121}$	$-\ell_2 \sqrt{2} m_e / v_d$	$-2.9 \cdot 10^{-5} \cdot \ell_2$
$\lambda_{122}$	$\ell_1 \sqrt{2} m_\mu / v_d$	$6.1 \cdot 10^{-3} \cdot \ell_1$
$\lambda_{123}$	0	0
$\lambda_{131}$	$-\ell_3 \sqrt{2} m_e / v_d$	$-2.9 \cdot 10^{-5} \cdot \ell_3$
$\lambda_{132}$	0	0
$\lambda_{133}$	$\ell_1 \sqrt{2} m_\tau / v_d$	$1.0 \cdot 10^{-1} \cdot \ell_1$
$\lambda_{231}$	0	0
$\lambda_{232}$	$-\ell_3 \sqrt{2} m_\mu / v_d$	$-6.1 \cdot 10^{-3} \cdot \ell_3$
$\lambda_{233}$	$\ell_2 \sqrt{2} m_\tau / v_d$	$1.0 \cdot 10^{-1} \cdot \ell_2$

TABLE I: Predictions for the  $LL\bar{E}$  in our ansatz as a function of the free parameters  $\ell_i$ .

Yukawa coupling matrices

$$\mathbf{U}_e^\dagger \cdot (\mathbf{h}^E)^T \cdot \mathbf{V}_e = \frac{\sqrt{2}}{v_d} \text{diag}(m_e, m_\mu, m_\tau), \quad (13)$$

$$\mathbf{U}_d^\dagger \cdot (\mathbf{h}^D)^T \cdot \mathbf{V}_d = \frac{\sqrt{2}}{v_d} \text{diag}(m_d, m_s, m_b), \quad (14)$$

$$\mathbf{U}_u^\dagger \cdot (\mathbf{h}^U)^T \cdot \mathbf{V}_u = \frac{\sqrt{2}}{v_u} \text{diag}(m_u, m_c, m_t), \quad (15)$$

where the normalization of the Higgs vacuum expectation value is  $v = \sqrt{|v_u|^2 + |v_d|^2} = 246 \text{ GeV}$  and  $\tan \beta \equiv v_u / v_d$ .

In the following, we assume that the charged lepton mass- and weak-eigenstates are the same. The corresponding charged lepton rotation matrices are then given by  $\mathbf{V}_e = \mathbf{U}_e = \mathbf{1}$ . Thus in our ansatz, in the leptonic sector the mixing takes place entirely in the neutrino sector, *cf.* the discussion in Refs. [61, 64]. Using Eqs. (8), and (13), the  $LL\bar{E}$  couplings can then be expressed in terms of the lepton masses and the three parameters  $\ell_i$

$$\lambda_{ijk} = \ell_i \frac{\sqrt{2} m_{ej}}{v_d} \delta_{jk} - \ell_j \frac{\sqrt{2} m_{ei}}{v_d} \delta_{ik}, \quad (16)$$

where  $m_{ej} \equiv (m_e, m_\mu, m_\tau)^j$ . Explicitly the couplings are given in Table I, as a function of the free parameters  $\ell_i$ . As an example, we have also given numerical coefficients in the case where  $\tan \beta = 10$ , which fixes  $v_d = 24.5 \text{ GeV}$ . Overall, of course, all couplings are proportional to the free parameters  $\ell_i$ .

We thus have some very specific predictions for the  $LL\bar{E}$  couplings in our model.

$$\lambda_{123} = \lambda_{132} = \lambda_{231} = 0 \quad (17)$$

$$\frac{\lambda_{121}}{\lambda_{233}} = -\frac{m_e}{m_\tau}, \quad \frac{\lambda_{122}}{\lambda_{133}} = \frac{m_\mu}{m_\tau}, \quad \frac{\lambda_{131}}{\lambda_{232}} = \frac{m_e}{m_\mu}. \quad (18)$$

Besides the vanishing couplings, we would thus expect

the couplings to satisfy the strict constraints

$$\lambda_{121} < 2.0 \cdot 10^{-5} \frac{m_{\tilde{\tau}_R}}{100 \text{ GeV}}, \quad (19)$$

$$\lambda_{122} < 3.6 \cdot 10^{-4} \sqrt{\frac{m_{\tilde{\tau}}}{100 \text{ GeV}}}, \quad (20)$$

$$\lambda_{131} < 3.4 \cdot 10^{-4} \frac{m_{\tilde{\mu}_R}}{100 \text{ GeV}}, \quad (21)$$

where we have implemented the low-energy bounds in [61] for  $\lambda_{133}$ ,  $\lambda_{233}$ ,  $\lambda_{232}$  and inserted the PDG lepton masses [65].

Throughout we consider our model only at the weak scale. In principle it should be embedded in a unified model at the grand unified scale or above [28, 29]. In that case, the predictions in Eqs. (17), (18) would be modified by renormalization group effects. In particular the couplings in Eq. (17) would get non-zero contributions [25], which however are extremely small, as they are proportional to the product of three non-zero  $LL\bar{E}$  couplings.

When expanding the  $LL\bar{E}$  term in the Lagrangian into its mass-eigenstate components, we obtain (summation over generation indices implied)

$$\begin{aligned} \mathcal{L}_{LL\bar{E}} = & \left[ -\lambda_{ijk} \tilde{e}_R^{k*} \tilde{\nu}^{ic} P_L e^j - \lambda_{ijk} \tilde{e}_L^j \tilde{e}^k P_L \nu^i \right. \\ & \left. - \lambda_{ijk} \tilde{\nu}_L^i \tilde{e}^k P_L e^j \right] + h.c.. \end{aligned} \quad (22)$$

Next we consider the  $LQ\bar{D}$  term in the Lagrangian.

Expanding out the  $SU(2)_L$  doublet superfields, we obtain

$$\mathcal{L}_{LQ\bar{D}} = \lambda'_{ijk} N_{Li} D_{Lj} \bar{D}_{Rk} - \lambda'_{ijk} E_{Li} U_{Lj} \bar{D}_{Rk}. \quad (23)$$

Rotating the quark superfields in the first term into the superfield basis where the quarks are in the mass-eigenstate and using Eqs. (9) and (13) we obtain

$$\begin{aligned} \lambda'_{ijk} N_{Li} D_{Lj} \bar{D}_{Rk} &= \lambda'_{ijk} [\mathbf{U}_d^\dagger]_{rk} [\mathbf{V}_d]_{js} N_{Li} D_{Ls}' \bar{D}'_{Rr} \\ &= \ell'_i [\mathbf{U}_d^\dagger (\mathbf{h}^D)^T \mathbf{V}_d]_{rs} N_{Li} D_{Ls}' \bar{D}'_{Rr} \\ &= \frac{\sqrt{2} \ell'_i}{v_d} m_{dr} \delta_{rs} N_{Li} D_{Ls}' \bar{D}'_{Rr}. \end{aligned} \quad (24)$$

For the second term in Eq.(23), we obtain analogously

$$\begin{aligned} \lambda'_{ijk} E_{Li} U_{Lj} \bar{D}_{Rk} &= \ell'_i [\mathbf{U}_d^\dagger (\mathbf{h}^D)^T \mathbf{V}_d]_{rt} [\mathbf{V}_d^\dagger \mathbf{V}_u]_{ts} E'_{Li} U_{Ls}' \bar{D}'_{Rr} \\ &= \frac{\sqrt{2} \ell'_i}{v_d} m_{dr} [\mathbf{V}^\dagger]_{sr} E'_{Li} U_{Ls}' \bar{D}'_{Rr}, \end{aligned} \quad (25)$$

where  $\mathbf{V}_{CKM} = \mathbf{V}_u^\dagger \mathbf{V}_d$  is the Cabibbo-Kobayashi-Maskawa matrix. Combining Eqs. (24) and (25), we can then write the Lagrangian for the  $LQ\bar{D}$  interactions in the mass-eigenstate basis and expanded in

superfield components<sup>1</sup>

$$\begin{aligned} \mathcal{L}_{LQ\bar{D}} &= \left[ -\tilde{\lambda}'_{ijk} \left( \tilde{\nu}_L^i \bar{d}^j P_L d^k + \tilde{d}_L^j \bar{d}^k P_L \nu^i + \tilde{d}_R^{j*} \bar{\nu}^{ic} P_L d^k \right) \right. \\ &\quad \left. + \tilde{\lambda}'_{ijk} V_{rj}^* \left( \tilde{e}_L^i \bar{d}^k P_L u^r + \tilde{u}_L^r \bar{d}^k P_L e^i + \tilde{d}_R^{k*} \bar{e}^{ic} P_L u^r \right) \right] \\ &\quad + h.c., \end{aligned} \quad (26)$$

with the coupling defined by

$$\tilde{\lambda}'_{ijk} \equiv \ell'_i \frac{\sqrt{2} m_{d_k}}{v_d} \delta_{jk}. \quad (27)$$

We also introduce the notation

$$\tilde{\tilde{\lambda}}'_{ijk} \equiv \ell'_i \frac{\sqrt{2} m_{d_k}}{v_d} [V]_{jk}. \quad (28)$$

Note that the (s)neutrino interactions are flavour diagonal in the down-(s)quarks, whereas the charged (s)lepton interactions involve generation off-diagonal (s)quark interactions [64]. We have given an estimate of the couplings  $\tilde{\lambda}'$  and  $\tilde{\tilde{\lambda}}'$ , modulo the  $\ell_i$  in Table II. We have again assumed  $\tan\beta = 10$ . Furthermore, we have taken the central PDG values for the quark masses:  $m_d = 6$  MeV,  $m_s = 103$  MeV,  $m_b = 4.2$  GeV, and the central values of the global PDG fit for the CKM matrix entries (2 significant figures) [65]

$$V_{CKM} = \begin{pmatrix} 0.97 & 0.23 & 0.0040 \\ 0.23 & 0.97 & 0.042 \\ 0.0081 & 0.042 & 1.0 \end{pmatrix}. \quad (29)$$

As can be seen from Table II, we thus have also simple predictions for the  $\tilde{\lambda}'$  couplings in terms of quark masses and  $V_{CKM}$  entries and independent of  $\tan\beta$ ,

$$\frac{\tilde{\lambda}'_{ijk}}{\tilde{\lambda}'_{ijl}} = \frac{m_{d_k} V_{jk}}{m_{d_l} V_{jl}}, \quad \frac{\tilde{\tilde{\lambda}}'_{ijk}}{\tilde{\tilde{\lambda}}'_{ilk}} = \frac{V_{jk}}{V_{lk}} \quad (30)$$

We can use Eqs. (16), (27) (28) to translate between our parameters  $\ell_i$ ,  $\ell'_i$  and the  $B_3$  couplings, where in the latter case, care must be taken to include the CKM-mixing for the charged (s)lepton interactions.

It is the purpose of this letter to investigate whether with this reduced freedom in the  $B_3$  sector, we can still obtain neutrino masses and mixings, which are, first of all, consistent with Eqs. (1)-(5) and second, where the resulting coupling constants are consistent with the existing low-energy bounds. In Sect. VIII, we then study possible observable consequences of the absolute values of the couplings as well as of the relative values.

Index	$\tilde{\lambda}'/\ell'_i$	$\tilde{\tilde{\lambda}}'/\ell'_i$
(i11)	$3.5 \cdot 10^{-4}$	$3.4 \cdot 10^{-4}$
(i12)	0	$1.4 \cdot 10^{-3}$
(i13)	0	$9.7 \cdot 10^{-4}$
(i21)	0	$8.0 \cdot 10^{-5}$
(i22)	$6.0 \cdot 10^{-3}$	$5.8 \cdot 10^{-3}$
(i23)	0	$1.0 \cdot 10^{-2}$
(i31)	0	$2.8 \cdot 10^{-6}$
(i32)	0	$2.5 \cdot 10^{-4}$
(i33)	0.24	0.24

TABLE II: Predictions for the  $LQ\bar{D}$  in our ansatz as a function of the free parameters  $\ell'_i$ . In the right column we have assumed  $\tan\beta = 10$ .

### III. OTHER ANSÄTZE

In Ref. [33, 34, 49] the hierarchy in the SM Higgs Yukawa couplings was taken to motivate a similar hierarchy in the  $LQ\bar{D}$  (and separately in the  $LL\bar{E}$  couplings). The authors restrict themselves to the couplings  $\lambda'_{i33}$  and  $\lambda_{i33}$ . We extend this interesting work in several respects. We include the most recent neutrino data in our fit; Eqs. (1)-(5). Furthermore, we include the CKM mixing in our ansatz, we thus have a prediction for the full range of the couplings. This is particularly important for the observable consequences of the model, *i.e.* the LSP decays. We also do combined fits including all the couplings, *i.e.* the  $\lambda$  and the  $\lambda'$  couplings and also the  $\kappa_i$ , our Models **I** and **II** below in Sect VI.

The most widely considered simple ansatz are  $B_3$  models, where  $\lambda_{ijk} = \lambda'_{ijk} = 0$  and  $\kappa_i \neq 0$ , often denoted bi-linear R-parity violation. This clearly has only three free parameters compared to the six or nine, in our models below. In order to compare the two ansätze in more detail, we combine the fields  $\mathcal{L}_\alpha = (\mathcal{L}_0, \mathcal{L}_i) = (H_d, L_i)$ , where  $\alpha = 0, \dots, 3$  and  $i = 1, 2, 3$ . The bi-linear R-parity violating superpotential is then

$$W = h_{ij}^E \mathcal{L}_i \mathcal{L}_0 \bar{E}_j + h_{ij}^D Q_i \mathcal{L}_0 \bar{D}_j + \mu \mathcal{L}_0 H_u + \kappa_i L_i H_u, \quad (31)$$

We can now make a field redefinition

$$\mathcal{L} \rightarrow \mathcal{L}' = \mathbf{R}\mathcal{L}, \quad (32)$$

such that the bi-linear lepton-number violating terms are eliminated from the superpotential. The explicit form for  $\mathbf{R}$  is given in Ref. [11, 18, 28]. We then obtain the superpotential

$$\begin{aligned} \tilde{W} &= h_{ij}^E [\mathbf{R}]_{i\alpha} [\mathbf{R}]_{0\beta} \mathcal{L}_\alpha \mathcal{L}_\beta \bar{E}_j \\ &\quad + h_{ij}^D [\mathbf{R}]_{0\alpha} Q_i \mathcal{L}_\alpha \bar{D}_j + \tilde{\mu} \mathcal{L}_0 H_u. \end{aligned} \quad (33)$$

The transformed parameters (denoted by a tilde) are

<sup>1</sup> The primes, denoting the mass-eigenstates, are omitted in the following.

then given by

$$\tilde{\mu} = \mu[\mathbf{R}]_{00} + \kappa_i[\mathbf{R}]_{i0} \quad (34)$$

$$\tilde{h}_{ij}^D = h_{ij}^D[\mathbf{R}]_{00} \quad (35)$$

$$\tilde{h}_{ij}^E = h_{ij}^E \left\{ [\mathbf{R}]_{li}[\mathbf{R}]_{00} - [\mathbf{R}]_{l0}[\mathbf{R}]_{0i} \right\} \quad (36)$$

$$\tilde{\lambda}'_{ijk} = h_{jk}^D[\mathbf{R}]_{0i} = \frac{[\mathbf{R}]_{0i}}{[\mathbf{R}]_{00}} \tilde{h}_{jk}^D \quad (37)$$

$$\begin{aligned} \tilde{\lambda}_{ijk} &= h_{lk}^E \left\{ [\mathbf{R}]_{lj}[\mathbf{R}]_{0i} - [\mathbf{R}]_{li}[\mathbf{R}]_{0j} \right\} \\ &= [\mathbf{R}]_{0i} \left( h_{lk}^E[\mathbf{R}]_{lj} \right) - [\mathbf{R}]_{0j} \left( [\mathbf{R}]_{li} h_{lk}^E \right). \end{aligned} \quad (38)$$

In the last equation we have included the parentheses to emphasize the sum over  $l$ . Note that not only are the tri-linear couplings  $\lambda_{ijk}$ ,  $\lambda'_{ijk}$  generated, but also the Higgs Yukawa couplings are modified

$$h_{ij}^{E,D} \longrightarrow \tilde{h}_{ij}^{E,D}. \quad (39)$$

From Eq. (37) we see that

$$\lambda'_{ijk} = \ell'_i \tilde{h}_{jk}^D, \quad \text{with} \quad \ell'_i = \frac{[\mathbf{R}]_{0i}}{[\mathbf{R}]_{00}} = \frac{\kappa_i}{\mu}. \quad (40)$$

In the last equation, we have employed the explicit form of the matrix  $\mathbf{R}$ . Next we would like to show that

$$\tilde{\lambda}_{ijk} = \ell_i \tilde{h}_{jk}^E - \ell_j \tilde{h}_{ik}^E. \quad (41)$$

For this we insert  $\tilde{h}^E$  from Eq. (36) and factor  $\ell_{i,j}$

$$\begin{aligned} \tilde{\lambda}_{ijk} &= \ell_j [\mathbf{R}]_{00} \left( h_{lk}^E[\mathbf{R}]_{li} \right) - \ell_i [\mathbf{R}]_{00} \left( h_{lk}^E[\mathbf{R}]_{lj} \right) \\ &+ \ell_j [\mathbf{R}]_{0i} \left( h_{lk}^E[\mathbf{R}]_{l0} \right) - \ell_i [\mathbf{R}]_{0j} \left( h_{lk}^E[\mathbf{R}]_{l0} \right) \end{aligned} \quad (42)$$

If we now set

$$\ell_i = \frac{[\mathbf{R}]_{0i}}{[\mathbf{R}]_{00}} \quad \text{and} \quad \ell_j = \frac{[\mathbf{R}]_{0j}}{[\mathbf{R}]_{00}}. \quad (43)$$

the last two terms in Eq. (42) cancel and the first two terms agree with Eq. (38). In particular, we see that  $B_3$  models with only bi-linear terms are a special case of our ansatz with  $\ell_i = \ell'_i$ .

#### IV. $B_3$ NEUTRINO MASSES

The general, lepton number violating superpotential in a  $B_3$ -model is given in Eq.(6). As stated in the introduction, due to the  $\kappa_i$ , the neutrinos mix with the Higgsino components of the neutralinos, resulting

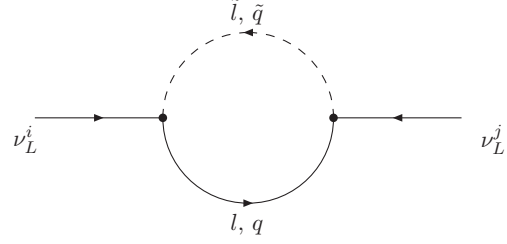


FIG. 1: The radiative slepton-lepton and squark-quark contribution to the neutrino mass.

in one massive neutrino at tree-level. The resulting mass matrix is perturbatively given by<sup>2</sup> [19, 20, 66]

$$\begin{aligned} (m_\nu^{\text{tree}})_{ij} &= \frac{m_Z^2 M_{\tilde{\gamma}} \cos^2 \beta}{\tilde{\mu} (m_Z^2 M_{\tilde{\gamma}} \sin 2\beta - M_1 M_2 \tilde{\mu})} \kappa_i \kappa_j, \\ &\equiv C_{\tilde{S}} \kappa_i \kappa_j. \end{aligned} \quad (44)$$

Here  $m_Z$  and  $M_{1,2}$  denote the mass of the  $Z^0$  gauge boson and the soft supersymmetry breaking, electroweak gaugino mass parameters, respectively. The photino mass is given by  $M_{\tilde{\gamma}} \equiv M_1 \cos^2 \theta_W + M_2 \sin^2 \theta_W$ , where  $\theta_W$  is the electroweak mixing angle.  $|\tilde{\mu}| \equiv \sqrt{\mu^2 + \sum_i |\kappa_i|^2}$ . We shall see below that  $\sum_i |\kappa_i|^2 = \mathcal{O}(1 \text{ MeV}^2)$  and thus to a high precision  $\tilde{\mu} \approx \mu$  [11, 19, 23]. For later convenience, we have introduced the constant  $C_{\tilde{S}}$  to summarize the dependence on the supersymmetric parameters. Within  $B_3$ -supersymmetry, the other two neutrinos obtain masses through radiative corrections from both the bi-linear [17, 18] and the tri-linear terms in the superpotential [19, 20]. In the following, we focus on the radiative corrections due to the tri-linear terms, since we expect these to dominate for small  $\kappa_i$  [11], however realistic neutrino mass models based only on bi-linear terms have been constructed [17, 18, 21].

There are two distinct radiative contributions to the neutrino masses from the tri-linear couplings for which the Feynman diagrams are shown in Fig. (1). One is proportional to  $\lambda'_{ik\ell} \lambda'_{j\ell k}$ , where a squark and a quark propagate in the loop. A second is given by a slepton-lepton loop, and is proportional to  $\lambda_{ik\ell} \lambda_{j\ell k}$ . For the squark-quark loop, the bottom-sbottom contribution dominates ( $k = \ell = 3$ ), since for the down-like quark masses we have  $m_b^2 \gg m_s^2, m_d^2$ . This results in the mass matrix<sup>3</sup>

$$(m_\nu^d)_{ij} \approx \frac{2N_c \lambda'_{i33} \lambda'_{j33}}{16\pi^2} m_b^2 A_b \frac{f(x_b)}{M_{\tilde{b}_2}^2}, \quad (45)$$

<sup>2</sup> As in [19], we assume here a rotation into the basis where the sneutrino vacuum expectation values vanish. In principle this requires a detailed minimization of the scalar potential as discussed for example in Ref. [11, 17, 21]. This is well beyond the scope of this paper.

<sup>3</sup> The extra factor of two arises from two distinct contributions to the mass which are equal for  $k = \ell$  [20].



where  $N_c = 3$  is the colour factor and

$$f(x_b) \equiv \frac{x_b \ln x_b}{x_b - 1}, \quad \text{with} \quad x_b = \left( \frac{M_{\tilde{b}_2}}{M_{\tilde{b}_1}} \right)^2. \quad (46)$$

$M_{\tilde{b}_s}$ ,  $s = 1, 2$ , denote the sbottom mass-eigenstates, where  $M_{\tilde{b}_1} < M_{\tilde{b}_2}$ .  $A_b \equiv A_b^0 - \bar{\mu} \tan \beta$ , where  $A_b^0$  is the tri-linear soft-supersymmetry breaking bottom coupling.  $i, j = 1, 2, 3$  are generation indices. In calculating explicit values for Eq. (45), the mixing of the left and right handed bottom squarks is taken into account but generation mixing is neglected due to the strict constraints from flavour changing neutral currents. For later numerical estimates, we find that

$$f(1) = 1, \quad f(100) \approx 4.65, \quad (47)$$

where the latter value corresponds to the fairly extreme value of  $M_{\tilde{b}_2} = 10 \cdot M_{\tilde{b}_1}$ . Note, there are no neutrino mass contributions proportional to  $m_b m_s$ . The subleading contribution is proportional to  $\lambda'_{i22} \lambda'_{j22} m_s^2$ . This could in principle be dominant for  $\lambda'_{i22} > (m_b/m_s) \lambda'_{i33} \approx 45 \cdot \lambda'_{i33}$ . However due to the relation Eq. (27), this is not possible in our ansatz, cf Table II.

The contribution from the slepton-lepton loop is analogously given by ( $N_c = 1$ )

$$(m_\nu^e)_{ij} \approx \frac{\lambda_{i33} \lambda_{j33}}{8\pi^2} m_\tau^2 A_\tau \frac{f(x_\tau)}{M_{\tilde{\tau}_2}^2}. \quad (48)$$

Here  $m_\tau$  is the tau mass and  $x_\tau = (M_{\tilde{\tau}_2}/M_{\tilde{\tau}_1})^2$ ,  $M_{\tilde{\tau}_1} < M_{\tilde{\tau}_2}$  are the stau masses.  $A_\tau \equiv A_\tau^0 - \bar{\mu} \tan \beta$ , where  $A_\tau^0$  is the trilinear soft breaking term for the  $\tau$ . Since  $\lambda_{ijk}$  is antisymmetric in the first two indices, we must restrict the indices  $i, j = 1, 2$  in Eq. (48). For  $i = j = 3$  the leading contribution<sup>4</sup> is from the smuon-muon loop, proportional to  $\lambda_{322}^2 m_\mu^2$ .

At any given energy scale, the mass parameters  $\kappa_i$  in Eq. (6) can be rotated away [67]. Depending on the scale and mechanism of supersymmetry breaking, the corresponding soft supersymmetry breaking terms will then also vanish [11]. When this occurs, we have pure tri-linear  $B_3$ -models, which have been widely discussed in the literature. The leading neutrino mass contributions must then arise solely from the above loop-diagrams. In the following, we shall thus discuss two models embedded in our ansatz. In Model **I**, we consider the case of pure tri-linear interactions, *i.e.*

<sup>4</sup> In principle, we could also have a contribution proportional to  $\lambda_{i22} \lambda_{j22} m_\mu^2 \propto \ell_3^2 m_\mu^4 / v_d^2$ . This can be large since  $\ell_3$  is a free parameter in our ansatz. However, in order to have a comparable contribution, we must have  $\ell_3 \approx (m_\tau / m_\mu)^2 \approx 300$ . Comparing with Table I, we see that the resulting  $\lambda_{232}$  typically violates the low-energy experimental bounds [61].

$\kappa_i = 0$ . The neutrino masses are then solely given through the combined loop contributions in Eqs. (45) and (48). In Model **II**, we consider the more general case with  $\kappa_i \neq 0$ , as well as  $\lambda, \lambda' \neq 0$ . In this case, either the complete Majorana neutrino mass matrix is given by the sum of all three contributions, Eqs. (44), (45) and (48) or one of the loop contributions is absent. In both models, the neutrino masses and mixing angles are then obtained upon diagonalization.

In the following, we shall first estimate the resulting neutrino masses in both Models **I** and **II** and then determine the masses and mixing angles by numerically diagonalising the complete mass matrix.

## V. NEUTRINO MASSES FROM THE SIMPLE $B_3$ -MODEL

We now insert our ansatz into the neutrino mass formulae above and give an estimate for the  $\ell_i, \ell'_j$ . The tree-level contribution, Eq. (44), is unchanged. The one-loop contributions, Eqs. (45) and (48), are given by

$$(\mathbf{M}_\nu^d)_{ij} \approx \frac{3\ell'_i \ell'_j m_b^4}{4\pi^2 v_d^2} A_b \frac{f(x_b)}{M_{b_2}^2} \equiv 3\ell'_i \ell'_j C_b, \quad (49)$$

$$(\mathbf{M}_\nu^e)_{ij} \approx \frac{\ell_i \ell_j m_\tau^4}{4\pi^2 v_d^2} A_\tau \frac{f(x_\tau)}{M_{\tau_2}^2} \equiv \ell_i \ell_j C_\tau, \quad (50)$$

where in the last equation  $i, j \neq 3$ . For later convenience we have introduced the constants  $C_{b,\tau}$ . In order to estimate the order of magnitude of the  $\ell_i, \ell'_j$ , we shall assume hierarchical neutrino masses. In Model **I**, the neutrino masses are generated alone from the loop corrections and the mass matrix is then

$$[\mathbf{M}_\nu]_{ij} = \ell_i \ell_j C_\tau + 3\ell'_i \ell'_j C_b, \quad (51)$$

which results in two massive neutrinos, since  $i, j \neq 3$  for  $C_\tau$ . We can obtain a third massive neutrino if we include the subleading term proportional to  $\ell_i \ell_j C_\mu$ , for which there is a contribution for  $i, j = 3$ .

In order to obtain an estimate, we set  $\tan \beta = 10$  and assume  $A_b^0 = A_\tau^0 = M_{\tilde{b},\tilde{\tau}} = m_{\text{soft}} = 100$  GeV, which results in  $f(x) \rightarrow 1$ . We then have  $C_b \approx 130$  keV and  $C_\tau = 4.1$  keV. The heaviest neutrino is in agreement with the atmospheric neutrino anomaly, Eq. (1), for

$$\ell \approx 3.5 \cdot 10^{-3}, \quad \text{or} \quad \ell' \approx 3.6 \cdot 10^{-4}, \quad (52)$$

$$\lambda_{i33} \approx 3.6 \cdot 10^{-4}, \quad \text{or} \quad \lambda'_{i33} \approx 8.7 \cdot 10^{-5}. \quad (53)$$

Correspondingly, we can generate the mass required by the solar neutrino anomaly by the other term. We obtain  $m_\nu \approx 0.01$  eV, for

$$\ell \approx 1.6 \cdot 10^{-3}, \quad \text{or} \quad \ell' \approx 1.6 \cdot 10^{-4}, \quad (54)$$

$$\lambda_{i33} \approx 1.6 \cdot 10^{-4}, \quad \text{or} \quad \lambda'_{i33} \approx 3.9 \cdot 10^{-5}, \quad (55)$$

For both the atmospheric and solar anomalies we have used Eqs. (16) and (27) to translate back to the corresponding values for  $\lambda_{i33}$  and  $\lambda'_{i33}$ .

In Model **II**, the largest neutrino mass is generated by the tree-level contribution. Taking the trace of Eq. (44), and assuming  $M_1 = M_2 = \mu = m_{soft}$ , we have approximately

$$m_\nu \approx \frac{m_Z^2 \cos^2 \beta \sum_i \kappa_i^2}{m_{soft}^3}. \quad (56)$$

From Eq. (1), we then obtain [23]

$$\sqrt{\sum \kappa_i^2} = \mathcal{O}(1 \text{ MeV}). \quad (57)$$

With the same assumptions as in Model **I**, the radiative contributions then generate the solar neutrino mass for the values given in Eqs. (54), (55).

## VI. NUMERICAL EVALUATION OF THE NEUTRINO MASSES

### A. General Outline

Next we wish to determine more precisely the parameters of our ansatz, *i.e.* the  $\ell_i, \ell'_i, \kappa_i$ , by fitting them to the neutrino data. They in turn fix the  $B_3$  parameters. In order to learn more about the importance of various parameters, we consider two cases. In Model **I**, we consider the case of pure tri-linear terms. The free parameters are

$$\text{Model I:} \quad \ell_i, \ell'_i. \quad (58)$$

In Model **II**, we include  $\kappa_i \neq 0$ ; the respective free parameters are given by

$$\text{Model II:} \quad \kappa_i, \ell_i, \ell'_i \quad (59)$$

Clearly, Model **II** is the most general case.

The full neutrino mass matrix  $(\mathbf{M}_\nu)_{ij}$  is given by the sum of Eqs. (44), (49) and (50), where depending on the model, the coefficient of  $C_{\tilde{S}}$  can be zero. In the case of Model **I**, the real symmetric mass matrix has the form of

$$\mathbf{M}_\nu^{\text{I}} = C_b \begin{pmatrix} \ell'_1 \ell'_1 & \ell'_1 \ell'_2 & \ell'_1 \ell'_3 \\ \ell'_2 \ell'_1 & \ell'_2 \ell'_2 & \ell'_2 \ell'_3 \\ \ell'_3 \ell'_1 & \ell'_3 \ell'_2 & \ell'_3 \ell'_3 \end{pmatrix} + C_\tau \begin{pmatrix} \ell_1 \ell_1 & \ell_1 \ell_2 & 0 \\ \ell_2 \ell_1 & \ell_2 \ell_2 & 0 \\ 0 & 0 & 0 \end{pmatrix}, \quad (60)$$

which is a function of five parameters. However, due to the simple form of the matrices, there are only two non-vanishing neutrino mass eigenvalues. This is sufficient to explain the atmospheric and solar neutrino anomalies. In principle, a massless lightest eigenstate

can also lead to an observable effect. If both the massless and the massive, second lightest neutrino have significant electron-neutrino admixtures, then the corresponding Kurie plot will have a dip at the electron energy  $Q - m_2$ , with  $m_2$  being the second lightest neutrino mass. The maximal electron energy however will be  $Q$ , within experimental uncertainties [68]. Depending on the parameter values this could be observable by the KATRIN experiment [69].

In Model **II**, we obtain three non-zero neutrino masses from the real symmetric mass matrix,

$$\mathbf{M}_\nu^{\text{II}} = C_{\tilde{S}} \begin{pmatrix} \kappa_1 \kappa_1 & \kappa_1 \kappa_2 & \kappa_1 \kappa_3 \\ \kappa_2 \kappa_1 & \kappa_2 \kappa_2 & \kappa_2 \kappa_3 \\ \kappa_3 \kappa_1 & \kappa_3 \kappa_2 & \kappa_3 \kappa_3 \end{pmatrix} + C_b \begin{pmatrix} \ell'_1 \ell'_1 & \ell'_1 \ell'_2 & \ell'_1 \ell'_3 \\ \ell'_2 \ell'_1 & \ell'_2 \ell'_2 & \ell'_2 \ell'_3 \\ \ell'_3 \ell'_1 & \ell'_3 \ell'_2 & \ell'_3 \ell'_3 \end{pmatrix} + C_\tau \begin{pmatrix} \ell_1 \ell_1 & \ell_1 \ell_2 & 0 \\ \ell_2 \ell_1 & \ell_2 \ell_2 & 0 \\ 0 & 0 & 0 \end{pmatrix}. \quad (61)$$

which depends on 8 independent parameters.

In the numerical evaluation, the coefficients  $C_{\tilde{S}}$ ,  $C_b$  and  $C_\tau$  are determined by assuming a BC1 mass spectrum [58], which has a scalar tau LSP. The resulting neutrino mass matrix  $(\mathbf{M}_\nu)_{ij}$  is diagonalized by the orthogonal rotation matrix  $\mathbf{V}$

$$\mathbf{V}^T \mathbf{M}_\nu \mathbf{V} = \begin{pmatrix} m_1 & 0 & 0 \\ 0 & m_2 & 0 \\ 0 & 0 & m_3 \end{pmatrix}, \quad (62)$$

where  $m_1 \leq m_2 \leq m_3$  and  $\mathbf{V}$  is given by the standard parameterization

$$\mathbf{V} = \begin{pmatrix} c_{12}c_{13} & s_{12}c_{13} & s_{13} \\ -s_{12}c_{23} - c_{12}s_{23}s_{13} & c_{12}c_{23} - s_{12}s_{23}s_{13} & s_{23}c_{13} \\ s_{12}s_{23} - c_{12}c_{23}s_{13} & -c_{12}s_{23} - s_{12}c_{23}s_{13} & c_{23}c_{13} \end{pmatrix}, \quad (63)$$

with  $c_{ij} = \cos \theta_{ij}$  and  $s_{ij} = \sin \theta_{ij}$ . The complex Dirac phase  $\delta_{13}$  and the two Majorana phases  $\alpha_{1/2}$  are omitted. The experimental ranges of the masses and the mixing parameters  $\theta_{12}$  and  $\theta_{23}$  are given in Eqs. (1)-(4). In addition, the bound on the mixing angle  $\theta_{13}$  from the CHOOZ experiment Eq. (5) is taken into account. We find it convenient in presenting our results instead of using the angles as in [6, 7], to use  $\tan^2 \theta_{12}$ ,  $\tan^2 \theta_{23}$  and  $\sin^2 \theta_{13}$ . The corresponding  $1\sigma$  ranges are given by

$$\tan^2 \theta_{12} \in [0.403, 0.490], \quad (64)$$

$$\tan^2 \theta_{23} \in [0.680, 1.20], \quad (65)$$

$$\sin^2 \theta_{13} < 0.0082. \quad (66)$$

In performing the fit, we randomly sample  $\log_{10}(\ell_i)$  and  $\log_{10}(\ell'_i)$ , thus guaranteeing that we explore the full hierarchy of couplings. We only consider couplings

$\ell_i, \ell'_j \geq 1 \cdot 10^{-7}$ , as smaller couplings have no effect on the neutrino observables. We furthermore require

$$\ell_i \ell_j \cdot C_\tau \leq 0.1 \text{ eV} \quad (67)$$

$$\ell'_i \ell'_j \cdot C_b \leq 0.1 \text{ eV} \quad (68)$$

$$\kappa_i \kappa_j \cdot C_S \leq 0.1 \text{ eV}. \quad (69)$$

For given values of the parameters  $\ell_i, \ell'_j, \kappa_k$ , the resulting mass matrix is computed. The numerical diagonalization of the mass matrix yields the mass eigen-

values  $m_1, m_2, m_3$  and the orthogonal transformation matrix  $V$  and thus the mixing angles  $\theta_{12}, \theta_{23}$  and  $\theta_{13}$ . Afterwards, all experimental requirements, Eqs. (1)-(5), are applied on the mass eigenvalues and on the mixing angles. We delete models, which do not fall within the  $1\sigma$  ranges. Throughout we also assume a hierarchical mass spectrum. Our results are summarized in Tables III and IV, which we discuss in the next section.

	$\ell_1$	$\ell_2$	$\ell'_1$	$\ell'_2$	$\ell'_3$	$\tan^2 \theta_{12}$	$\tan^2 \theta_{23}$	$\sin^2 \theta_{13}$	$\Delta m_{21}^2$	$\Delta m_{23}^2$
$\ell_1$ max	$9.38 \cdot 10^{-4}$	$1.69 \cdot 10^{-3}$	$-1.60 \cdot 10^{-7}$	$4.01 \cdot 10^{-4}$	$-5.22 \cdot 10^{-4}$	0.48	0.99	0.0078	0.081	2.5
$\ell_1$ min	$7.10 \cdot 10^{-4}$	$-1.76 \cdot 10^{-3}$	$9.27 \cdot 10^{-5}$	$4.16 \cdot 10^{-4}$	$-5.09 \cdot 10^{-4}$	0.42	1.10	0.0037	0.077	2.6
$\ell_2$ max	$-7.12 \cdot 10^{-4}$	$1.78 \cdot 10^{-3}$	$-9.42 \cdot 10^{-5}$	$-4.10 \cdot 10^{-4}$	$5.04 \cdot 10^{-4}$	0.42	1.11	0.0038	0.081	2.5
$\ell_2$ min	$9.23 \cdot 10^{-4}$	$1.58 \cdot 10^{-3}$	$1.82 \cdot 10^{-6}$	$3.83 \cdot 10^{-4}$	$-5.60 \cdot 10^{-4}$	0.49	0.72	0.0056	0.078	2.7
$\ell'_1$ max	$7.10 \cdot 10^{-4}$	$-1.76 \cdot 10^{-3}$	$9.27 \cdot 10^{-5}$	$4.16 \cdot 10^{-4}$	$-5.09 \cdot 10^{-4}$	0.42	1.10	0.0037	0.077	2.6
$\ell'_1$ min	$-9.14 \cdot 10^{-4}$	$-1.67 \cdot 10^{-3}$	$1.00 \cdot 10^{-7}$	$4.11 \cdot 10^{-4}$	$-5.35 \cdot 10^{-4}$	0.47	0.95	0.0065	0.077	2.7
$\ell'_2$ max	$9.01 \cdot 10^{-4}$	$-1.77 \cdot 10^{-3}$	$1.10 \cdot 10^{-7}$	$4.28 \cdot 10^{-4}$	$5.16 \cdot 10^{-4}$	0.43	1.18	0.0077	0.078	2.8
$\ell'_2$ min	$8.73 \cdot 10^{-4}$	$1.62 \cdot 10^{-3}$	$4.00 \cdot 10^{-7}$	$3.61 \cdot 10^{-4}$	$-5.53 \cdot 10^{-4}$	0.41	0.68	0.0053	0.080	2.4
$\ell'_3$ max	$8.69 \cdot 10^{-4}$	$1.61 \cdot 10^{-3}$	$-5.50 \cdot 10^{-7}$	$3.82 \cdot 10^{-4}$	$5.71 \cdot 10^{-4}$	0.42	0.69	0.0043	0.078	2.8
$\ell'_3$ min	$-7.12 \cdot 10^{-4}$	$1.78 \cdot 10^{-3}$	$-9.42 \cdot 10^{-5}$	$-4.10 \cdot 10^{-4}$	$5.04 \cdot 10^{-4}$	0.42	1.11	0.0038	0.081	2.5

TABLE III: Explicit solutions for Model **I**, where  $\kappa_i = 0$ . We only show the values where one of the  $|\ell_i|, |\ell'_j|$  takes on an extremal absolute value, *i.e.* the highest or lowest value obtained in our fits. Note that due to our sampling constraints, we did not probe values for the  $\ell_i, \ell'_j < 10^{-7}$ . In the five columns on the far right, we show the resulting neutrino parameters. The values for  $\Delta m_{21}^2$  and  $\Delta m_{23}^2$  are given units  $10^{-3} \text{ eV}^2$ . Comparing with Eqs. (1)-(5), we can see which physical parameter is at its experimentally allowed limit. Thus for example in the first row, where  $\ell_1$  is maximal,  $\tan^2 \theta_{12}$  and  $\Delta m_{21}^2$  are at the edge of their allowed values. Pushing  $\ell_1$  any higher would violate these constraints.

	$\ell_1$	$\ell_2$	$\ell'_1$	$\ell'_2$	$\ell'_3$	$\kappa_1$	$\kappa_2$	$\kappa_3$
$\ell_1$ max	$1.08 \cdot 10^{-3}$	$-1.17 \cdot 10^{-3}$	$1.80 \cdot 10^{-6}$	$-4.39 \cdot 10^{-4}$	$4.57 \cdot 10^{-4}$	-0.128	0.00551	-3.40
$\ell_1$ min	$1.30 \cdot 10^{-7}$	$1.45 \cdot 10^{-5}$	$-6.50 \cdot 10^{-7}$	$-4.30 \cdot 10^{-4}$	$5.35 \cdot 10^{-4}$	1.93	2.82	1.09
$\ell_2$ max	$-8.15 \cdot 10^{-4}$	$1.77 \cdot 10^{-3}$	$4.06 \cdot 10^{-5}$	$4.14 \cdot 10^{-4}$	$-5.01 \cdot 10^{-4}$	-0.159	-0.541	-0.103
$\ell_2$ min	$4.50 \cdot 10^{-7}$	$1.20 \cdot 10^{-7}$	$1.42 \cdot 10^{-4}$	$3.22 \cdot 10^{-4}$	$4.10 \cdot 10^{-7}$	1.02	-4.65	6.11
$\ell'_1$ max	$-8.80 \cdot 10^{-7}$	$1.34 \cdot 10^{-3}$	$1.84 \cdot 10^{-4}$	$2.28 \cdot 10^{-4}$	$2.20 \cdot 10^{-6}$	0.401	-4.64	6.01
$\ell'_1$ min	$-4.65 \cdot 10^{-6}$	$9.62 \cdot 10^{-6}$	$2.20 \cdot 10^{-7}$	$-5.28 \cdot 10^{-4}$	$-4.04 \cdot 10^{-4}$	-2.07	-0.0320	3.72
$\ell'_2$ max	$-1.50 \cdot 10^{-6}$	$-7.07 \cdot 10^{-6}$	$-8.85 \cdot 10^{-5}$	$5.31 \cdot 10^{-4}$	$-4.10 \cdot 10^{-4}$	1.70	0.100	-3.81
$\ell'_2$ min	$-9.49 \cdot 10^{-4}$	$1.66 \cdot 10^{-3}$	$-9.70 \cdot 10^{-6}$	$1.30 \cdot 10^{-7}$	$1.10 \cdot 10^{-4}$	0.219	4.92	5.98
$\ell'_3$ max	$8.82 \cdot 10^{-4}$	$1.64 \cdot 10^{-3}$	$3.60 \cdot 10^{-7}$	$3.91 \cdot 10^{-4}$	$5.55 \cdot 10^{-4}$	-0.457	0.0604	-0.218
$\ell'_3$ min	$4.50 \cdot 10^{-7}$	$1.20 \cdot 10^{-7}$	$1.42 \cdot 10^{-4}$	$3.22 \cdot 10^{-4}$	$4.10 \cdot 10^{-7}$	1.02	-4.65	6.11
$\kappa_1$ max	$1.43 \cdot 10^{-4}$	$-1.30 \cdot 10^{-3}$	$-2.69 \cdot 10^{-6}$	$4.47 \cdot 10^{-4}$	$-4.77 \cdot 10^{-4}$	2.06	-0.0125	-3.03
$\kappa_1$ min	$-1.87 \cdot 10^{-6}$	$-2.30 \cdot 10^{-5}$	$-1.74 \cdot 10^{-4}$	$-4.23 \cdot 10^{-5}$	$2.99 \cdot 10^{-4}$	0.0149	-5.90	-5.32
$\kappa_2$ max	$1.21 \cdot 10^{-4}$	$3.77 \cdot 10^{-5}$	$-1.65 \cdot 10^{-4}$	$-1.04 \cdot 10^{-4}$	$2.27 \cdot 10^{-4}$	0.139	6.18	5.26
$\kappa_2$ min	$9.03 \cdot 10^{-4}$	$-1.19 \cdot 10^{-3}$	$-2.15 \cdot 10^{-5}$	$4.56 \cdot 10^{-4}$	$-4.49 \cdot 10^{-4}$	-0.556	0.0338	3.16
$\kappa_3$ max	$-7.67 \cdot 10^{-4}$	$-1.23 \cdot 10^{-3}$	$-8.03 \cdot 10^{-5}$	$-1.07 \cdot 10^{-4}$	$1.31 \cdot 10^{-4}$	-0.0348	5.00	6.42
$\kappa_3$ min	$9.00 \cdot 10^{-4}$	$-1.60 \cdot 10^{-3}$	$2.30 \cdot 10^{-6}$	$-3.75 \cdot 10^{-4}$	$-5.64 \cdot 10^{-4}$	0.0656	-0.0242	0.0140

TABLE IV: The same as Table III for Model **II**. Now we also have the values of  $\kappa_i$  as well as the extremal values of  $|\kappa_i|$ . The  $\kappa_i$  are given in units of MeV.



	$\tan^2 \theta_{12}$	$\tan^2 \theta_{23}$	$\sin^2 \theta_{13}$	$\Delta m_{21}^2$	$\Delta m_{23}^2$
$\ell_1$ max	0.48	0.80	0.0061	0.077	2.4
$\ell_1$ min	0.45	0.79	0.0012	0.081	2.5
$\ell_2$ max	0.41	1.19	0.0007	0.078	2.5
$\ell_2$ min	0.44	0.93	0.0031	0.080	2.4
$\ell'_1$ max	0.41	1.06	0.0003	0.079	2.4
$\ell'_1$ min	0.47	1.04	0.0072	0.081	2.6
$\ell'_2$ max	0.44	1.03	0.0009	0.080	2.7
$\ell'_2$ min	0.47	1.04	0.0075	0.080	2.6
$\ell'_3$ max	0.44	0.78	0.0053	0.079	2.7
$\ell'_3$ min	0.44	0.93	0.0031	0.080	2.4
$\kappa_1$ max	0.40	0.83	0.0034	0.080	2.6
$\kappa_1$ min	0.47	0.81	0.0056	0.081	2.7
$\kappa_2$ max	0.49	1.18	0.0001	0.078	2.6
$\kappa_2$ min	0.42	0.95	0.0051	0.081	2.4
$\kappa_3$ max	0.44	0.74	0.0014	0.081	2.8
$\kappa_3$ min	0.45	0.69	0.0055	0.080	2.6

TABLE V: Model **II** (continued). Again, the values for  $\Delta m_{21}^2$  and  $\Delta m_{23}^2$  are given units  $10^{-3} \text{ eV}^2$ .

## B. Discussion of the Results

### 1. Model I

In Table III, we present the fit values for the parameters  $\ell_i, \ell'_j$  in Model **I**. In the five columns on the right, we also include the resulting neutrino mass and mixing parameters. Of the large number of solutions we find, we present those where the parameters  $|\ell_i|$  take on extremal values. For example in the first row of Table III,  $|\ell_1|$  takes on the largest value we have found. We can now see in the five columns on the right, that  $\tan^2 \theta_{12}$  and  $\Delta m_{21}^2$ , are at the upper limit of their allowed ranges, Eqs. (1) and (64), respectively. This is as we would expect from Eq. (61), where we see that  $\ell_1$  influences the first two generations. On the other hand, for example in the seventh row, where  $|\ell'_2|$  is maximal, we see that  $\tan^2 \theta_{23}$  and  $\Delta m_{32}^2$  are at the upper limit of their allowed ranges. Similarly, in the second row, where  $|\ell_1|$  is minimal, we see that  $\Delta m_{21}^2$  is at the *lower* end of its allowed range. For the eighth row, where  $|\ell'_2|$  is minimal,  $\Delta m_{32}^2$  is at the *lower* end of its allowed range. Overall, we see that  $\tan^2 \theta_{12}$  is at its upper limit for  $[\ell_1 \text{ max}]$  and also for  $[\ell_2 \text{ min}]$ .  $\tan^2 \theta_{23}$  is at its upper limit for  $[\ell'_2 \text{ max}]$  and at its lower limit for  $[\ell'_2 \text{ min}]$  and  $[\ell'_3 \text{ max}]$ .  $\sin^2 \theta_{13}$  is always well within its limits and thus does not pose a real constraint on our fit. However, we do predict a value between 0.003 and the current upper bound. For  $\Delta m_{21}^2$ , we are at the upper end of the allowed range for  $[\ell_1 \text{ max}]$ ,  $[\ell_2 \text{ max}]$ , and  $[\ell'_3 \text{ min}]$ . We are close to the lower range for  $[\ell_1 \text{ min}]$ ,  $[\ell'_1 \text{ max}]$ , and  $[\ell'_1 \text{ min}]$ . For  $\Delta m_{23}^2$ , we are at the upper end of the allowed range for  $[\ell'_2 \text{ max}]$  and

$[\ell'_3 \text{ max}]$ . Thus we get the strongest constraints from the allowed mass ranges and from  $\tan^2 \theta_{23}$ .

In the case of Model **I**, we only have five free parameters. With these we must fit the two neutrino masses, two mixing angles and one upper bound. It is thus perhaps not surprising, that except for  $\ell'_1$ , the allowed ranges for the five parameters are quite narrow.  $\ell'_{1 \text{ min}}$  is consistent with zero. In summary, we find from Table III

$$7.10 \cdot 10^{-4} < |\ell_1| < 9.38 \cdot 10^{-4} \quad (70)$$

$$1.58 \cdot 10^{-3} < |\ell_2| < 1.78 \cdot 10^{-3} \quad (71)$$

$$1.00 \cdot 10^{-7} < |\ell'_1| < 9.27 \cdot 10^{-5} \quad (72)$$

$$3.61 \cdot 10^{-4} < |\ell'_2| < 4.28 \cdot 10^{-4} \quad (73)$$

$$5.04 \cdot 10^{-4} < |\ell'_3| < 5.71 \cdot 10^{-4}. \quad (74)$$

We shall employ the central values of these regions in the discussion of the resulting collider signals, below.

### 2. Model II

In Table IV, we show the results of our fit to Model **II**. We now have a total of eight free-parameters. We vary the values of the mass mixing parameters in the interval

$$0.01 \text{ MeV} \leq \kappa_i \leq 10 \text{ MeV}. \quad (75)$$

Due to the enhanced freedom, we see that we now have solutions, where are proportionality constants  $\ell_i, \ell'_j = \mathcal{O}(10^{-7})$ , which is consistent with zero, in our approach. We see that we push the upper boundary of  $\tan^2 \theta_{12}$  for  $[\ell_1 \text{ max}]$  and  $[\kappa_2 \text{ max}]$  and the lower boundary for  $[\kappa_1 \text{ max}]$ . For  $\tan^2 \theta_{23}$  we push the upper and lower limits for  $[\kappa_2 \text{ max}]$  and for  $[\kappa_3 \text{ min}]$ , respectively. From  $\sin^2 \theta_{13}$ , we again have basically no constraint on our model, beyond those of the other parameters, *i.e.* we are always well within the CHOOZ bound.

We are pushing the upper end of the allowed range of  $\Delta m_{21}^2$  for  $[\ell_1 \text{ min.}]$ ,  $[\ell'_1 \text{ min.}]$ ,  $[\kappa_{1,2} \text{ min.}]$ , and  $[\kappa_3 \text{ max.}]$ . For  $\Delta m_{23}^2$ , we are at the upper end for  $[\ell'_2 \text{ max.}]$ ,  $[\ell'_3 \text{ max.}]$ , and  $[\kappa_1 \text{ min.}]$ . We are at the *lower* end of  $\Delta m_{23}^2$  for  $[\ell_1 \text{ max.}]$ ,  $[\ell_2 \text{ min.}]$ ,  $[\ell'_1 \text{ max.}]$ ,  $[\ell'_3 \text{ min.}]$ , and  $[\kappa_2 \text{ min.}]$ . Thus the mass ranges set the strictest limits on our parameters, the angles are fairly easy to accommodate.

Due to the enhanced freedom, we see that any one of our parameters can consistently be set to zero. This is of particular interest when trying to extract typical collider signatures, below. In Model **II**, it is thus difficult to discern an identifying experimental signature.

	$\lambda_{122}\lambda'_{211}$	$\lambda_{132}\lambda'_{311}$	$\lambda_{121}\lambda'_{111}$	$\lambda_{231}\lambda'_{311}$
Bound	$4.0 \cdot 10^{-8}$	$4.0 \cdot 10^{-8}$	$4.0 \cdot 10^{-8}$	$4.0 \cdot 10^{-8}$

	$\lambda'_{i12}\lambda'_{i21}$	$\lambda'_{i13}\lambda'_{i31}$	$\lambda'_{i13}\lambda'_{i31}$	$\lambda'_{1k1}\lambda'_{2k1}$	$\lambda'_{11j}\lambda'_{21j}$
Bound	$10^{-9}$	$3 \cdot 10^{-8}$	$8 \cdot 10^{-8}$	$8.0 \cdot 10^{-8}$	$8.5 \cdot 10^{-8}$

TABLE VI: Bounds on the products of  $B_3$  couplings [61]. The first four and the last two bounds arise from contributions to the process  $\mu\text{Ti} \rightarrow e\text{Ti}$ . The fifth bound arises from contributions to  $\Delta m_K$  and the sixth and seventh from contributions to  $\Delta m_B$ .

## VII. BOUNDS ON THE PRODUCTS OF THE PARAMETERS OF THE SIMPLE $B_3$ -MODEL

Before discussing the consequences of our model, we first consider the low-energy constraints. Typical bounds on single  $B_3$  couplings are of order 0.1 to 0.01 [15, 70]. However, we necessarily have multiple couplings in our models and thus must take into account the bounds on products of couplings [59, 60, 61, 62], which are also typically much stricter, due to lepton flavor violating effects. The strictest product bounds ( $< 10^{-7}$ ) of Table II in Ref. [61] are given in Table VI.

We can now investigate whether our couplings satisfy the bounds in Table VI. For this we use the values in Tables I and II and assume  $\tan\beta = 10$ . We find

$$\lambda_{122}\lambda'_{211} = 2.1 \cdot 10^{-6} \ell_1 \ell'_2 \quad (76)$$

$$\lambda_{132}\lambda'_{311} = 0 \quad (77)$$

$$\lambda_{121}\lambda'_{111} = -9.9 \cdot 10^{-9} \ell_2 \ell'_1 \quad (78)$$

$$\lambda_{231}\lambda'_{311} = 0 \quad (79)$$

$$\lambda'_{i12}\lambda'_{i21} = 1.1 \cdot 10^{-7} (\ell'_i)^2 \quad (80)$$

$$\lambda'_{113}\lambda'_{131} = 2.7 \cdot 10^{-9} (\ell'_1)^2 \quad (81)$$

$$\lambda'_{i13}\lambda'_{i31} = 2.7 \cdot 10^{-9} (\ell'_i)^2 \quad (82)$$

$$\lambda'_{1k1}\lambda'_{2k1} = 1.2 \cdot 10^{-7} \ell'_1 \ell'_2, \quad k = 1 \quad (83)$$

$$\lambda'_{11j}\lambda'_{21j} = 2.0 \cdot 10^{-6} \ell'_1 \ell'_2, \quad j = 2 \quad (84)$$

In the last two cases the chosen indices result in the largest possible value. The strictest bounds result from Eqs. (76) and (80):  $\ell_1 \ell'_2 < 0.02$ , and  $\ell'_i < 0.1$ . From Tables III and IV, we see that these are always satisfied in our numerical solutions.

## VIII. COLLIDER TESTS

An essential feature of  $B_3$  neutrino models, is that they necessarily lead to observable consequences at colliders. Resonant slepton or squark production requires couplings of order  $10^{-3}$  or larger [57]. As can be seen from Tables I and II together with the numerical results presented in Tables III, IV, this is not possible in our models. However, it is well known, that at the LHC squark and gluino production provide the largest

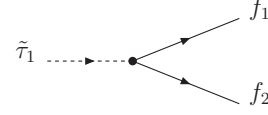


FIG. 2: The two-body decay of a scalar particle into two fermions.

supersymmetric cross sections. This is independent of whether  $P_6$  or  $B_3$  is the relevant symmetry. The produced squarks and gluinos then cascade decay within the detector to the LSP. In particular, this also holds for the BC benchmark points [58], where  $\tilde{\tau}_1$  is the LSP. In this paper, we focus on stau-LSP scenarios, as outlined in Ref. [58]. We shall focus on the essential features, a full phenomenological analysis goes beyond the scope of this paper and will be presented elsewhere [71]. The neutralino LSP case requires a full treatment of the scalar potential in order to determine the relevant couplings and masses. This in turn requires assumptions about the soft-supersymmetry breaking sector, which also goes well beyond the scope of this paper. We shall consider this elsewhere [71].

### A. Stau LSP Decays

As discussed in detail in Refs. [11, 58], there are extensive regions of mSUGRA parameter space, where the scalar tau is the LSP. The final state collider signals will be determined by the dominant decays of the stau. The lightest stau,  $\tilde{\tau}_1$ , is an admixture of right and left stau.

$$\tilde{\tau}_1 = \cos\theta_{\tilde{\tau}} \tilde{\tau}_R + \sin\theta_{\tilde{\tau}} \tilde{\tau}_L \quad (85)$$

with  $\theta_{\tilde{\tau}}$  the mixing angle. In Ref. [58], it was found that in the representative benchmark points (BC1-BC4) the  $\tilde{\tau}_1$  is dominantly a right-handed stau with  $|\theta_{\tilde{\tau}}| < 0.3$  (in radians), *i.e.* the  $\tilde{\tau}_1$ -LSP is more than 91%  $\tilde{\tau}_R$  and  $\sin^2\theta_{\tilde{\tau}} < 0.09$ .

In our model, we have a wide range of non-zero  $B_3$  couplings, where the corresponding operators couple directly to the stau. The stau can thus decay via the two-body mode into two spin-1/2 fermions  $f_{1,2}$  shown in Fig. 2. The corresponding partial decay rate is in given in leading order by [72]

$$\Gamma(\tilde{\tau}_1 \rightarrow f_1 f_2) = \frac{N_c |\Lambda|^2 \Theta^2 p_{cm}}{8\pi M_{\tilde{\tau}_1}^2} (M_{\tilde{\tau}_1}^2 - m_1^2 - m_2^2) \quad (86)$$

$$\approx \frac{N_c |\Lambda|^2 \Theta^2}{16\pi} M_{\tilde{\tau}_1}, \quad (87)$$

where

$$p_{cm}^2 = \frac{[M_{\tilde{\tau}_1}^2 - (m_1 + m_2)^2][M_{\tilde{\tau}_1}^2 - (m_1 - m_2)^2]}{4M_{\tilde{\tau}_1}^2}. \quad (88)$$

Operator	Decay Mode	$\Gamma(\tilde{\tau}_1^- \rightarrow bc)/M_{\tilde{\tau}_1}$
$L_1 L_3 \bar{E}_1$	$\tilde{\tau}_1^- \rightarrow e^- \nu_e$	$1.5 \cdot 10^{-12} \ell_3^2$
$L_1 L_3 \bar{E}_3$	$\tilde{\tau}_1^- \rightarrow \tau^- \nu_e$	$2.0 \cdot 10^{-4} \ell_1^2$
$L_1 L_3 \bar{E}_2$	$\tilde{\tau}_1^- \rightarrow e^- \nu_\tau$	$1.8 \cdot 10^{-4} \ell_1^2$
$L_2 L_3 \bar{E}_2$	$\tilde{\tau}_1^- \rightarrow \mu^- \nu_\mu$	$6.7 \cdot 10^{-8} \ell_3^2$
$L_2 L_3 \bar{E}_3$	$\tilde{\tau}_1^- \rightarrow \tau^- \nu_\mu$	$2.0 \cdot 10^{-4} \ell_2^2$
$L_2 L_3 \bar{E}_1$	$\tilde{\tau}_1^- \rightarrow \mu^- \nu_\tau$	$1.8 \cdot 10^{-4} \ell_2^2$
$L_3 Q_2 \bar{D}_3$	$\tilde{\tau}_1^- \rightarrow cb$	$5.4 \cdot 10^{-7} (\ell'_3)^2$
$L_3 Q_2 \bar{D}_2$	$\tilde{\tau}_1^- \rightarrow cs$	$1.8 \cdot 10^{-7} (\ell'_3)^2$
$L_3 Q_1 \bar{D}_2$	$\tilde{\tau}_1^- \rightarrow us$	$1.1 \cdot 10^{-8} (\ell'_3)^2$

TABLE VII: Decay modes and partial decay widths of a stau LSP given as a function of the relevant  $\ell_i, \ell'_j$ . In the second and the fifth decay modes we have added the two contributions from the doublet and the singlet stau. We have set  $\theta_\tau = 0.3$  (in radians) as obtained for BC1.

$m_{1,2}$  denote the final state masses.  $\Lambda$  denotes one of the following  $B_3$  couplings relevant for tree-level stau decay

$$\Lambda \in \{\lambda_{131}, \lambda_{133}, \lambda_{232}, \lambda_{233}, \lambda'_{3jk}\}, \quad (89)$$

and  $N_c$  is the colour factor.  $N_c = 1$  for the decay via the  $LL\bar{E}$  operators, and  $N_c = 3$  for the  $LQ\bar{D}$  operators.  $\Theta = (\cos \theta_\tau, \sin \theta_\tau)$ , depending on whether the  $\tilde{\tau}_1$  couples via the right- or the left-handed stau component. Eq. (87) is taken for the case where  $m_{1,2} \rightarrow 0$ . This is a good approximation for  $M_{\tilde{\tau}_1} < m_{\text{top}}$ , which is the case for all the BC benchmark points.

Given the above decay formula we can now compute the decay rates for the dominant decay modes using the numerical values in Tables I and II for the relevant coupling. We expect the decays where the right-handed stau component couples directly to dominate, due to the small mixing angle in the stau sector. Furthermore, for  $\lambda'_{333}$  which is a potentially large coupling the large top quark mass kinematically blocks the decay, for the stau masses we consider here. We present the results for the decays in terms of the  $\ell_i, \ell'_j$  in Table VII. For completeness, we have included the couplings involving  $\ell_3$ , which we have neglected in our neutrino parameter fits. We see that for substantial decays via the corresponding operators, we would require, *e.g.*  $\ell_3 \gg \ell_{1,2}$ .

### 1. Model I

If we consider the BC1 benchmark point, we have  $M_{\tilde{\tau}_1} = 148.38$  GeV. Using Tables III, IV we can then compute explicit values for the partial widths and the branching ratios. In Model I,  $|\ell_1| \approx 8 \cdot 10^{-4}$ ,  $|\ell_2| \approx 2 \cdot 10^{-3}$  and  $|\ell'_3| \approx 5 \cdot 10^{-4}$ . Using these values, we then obtain the total decay width and lifetime in Model I at BC1

$$\Gamma(\tilde{\tau}_1) = 260 \text{ eV}, \quad \tau(\tilde{\tau}_1) = 2.5 \cdot 10^{-18} \text{ sec.} \quad (90)$$

We see that the stau-LSP always decays within the detector. It also will not lead to a detached vertex. For the branching ratios of the decay modes in Table VII, we obtain

$$\text{Br}(\tilde{\tau}_1 \rightarrow \tau^- \nu_e) = 0.072 \quad (91)$$

$$\text{Br}(\tilde{\tau}_1 \rightarrow e^- \nu_\tau) = 0.065 \quad (92)$$

$$\text{Br}(\tilde{\tau}_1 \rightarrow \tau^- \nu_\mu) = 0.45 \quad (93)$$

$$\text{Br}(\tilde{\tau}_1 \rightarrow \mu^- \nu_\tau) = 0.41 \quad (94)$$

The other decay modes are negligible. The branching ratios are independent of  $M_{\tilde{\tau}_1}$ , *i.e.* in Model I they only depend on the  $\ell_i, \ell'_j$ . As the neutrinos are not visible, we have a combined branching ratio into charged tau leptons of about 52%. For squark or gluino pair production, we expect two stau's in the decay chains. The probability for then having two charged electrons/muons in the final state is about 23%. Since the gluino/squark pair production cross section is very large for accessible supersymmetric masses, this should lead to an easily visible signal rate.

### 2. Model II

In Model II, we have eight free parameters and thus a much larger freedom. Furthermore for  $\kappa_3 \neq 0$  the stau can mix with the charged Higgs boson, leading to additional decay modes. In order to compute these properly, we must minimize the full scalar potential. This is beyond the scope of this paper. We can estimate the stau-Higgs mixing to be  $\kappa_3/\mu$ . Using the Feynman rules in Fig. 8 of Ref. [73] for the charged Higgs coupling to the tau lepton, we then typically find a product of mixing times couplings of order  $10^{-7}$ , for  $\kappa_3 = 1$  MeV,  $\tan \beta = 10$  and  $\mu = 200$  GeV. This would lead to an additional decay  $\tilde{\tau} \rightarrow \tau \nu$ . The couplings to the second generation quarks are another order of magnitude smaller. These Higgs-mixing couplings are negligible compared to the direct stau decay couplings, in most cases. However, in general they must be included. A proper complete treatment will be given in Ref. [71]. Here it shall suffice to present one example case from Table IV employing only the direct decays from Table VII. We choose the example, such that  $\ell_{1,2} \ll \ell'_3$ , which differs from Model I.

We consider the case:  $[\ell'_1 \text{ min}]$ , where  $\ell_1 = -4.65 \cdot 10^{-6}$ ,  $\ell_2 = 9.62 \cdot 10^{-6}$  and  $\ell'_3 = -4.04 \cdot 10^{-4}$ . We find for the total decay rate and the lifetime

$$\Gamma(\tilde{\tau}_1) = 2.4 \cdot 10^{-2} \text{ eV}, \quad (95)$$

$$\tau(\tilde{\tau}_1) = 2.7 \cdot 10^{-14} \text{ sec.} \quad (96)$$

We see that the width is now substantially smaller and thus the lifetime correspondingly larger. For a Lorentz boost  $\gamma_L = 10$ , we have a decay length of about  $100 \mu\text{m}$ . This is on the borderline of visibility

for a detached vertex. For the branching ratios we find

$$\text{Br}(\tilde{\tau}_1 \rightarrow \text{hadrons}) = 0.73 \quad (97)$$

$$\text{Br}(\tilde{\tau}_1 \rightarrow \tau^- \nu_e) = 0.026 \quad (98)$$

$$\text{Br}(\tilde{\tau}_1 \rightarrow e^- \nu_\tau) = 0.023 \quad (99)$$

$$\text{Br}(\tilde{\tau}_1 \rightarrow \tau^- \nu_\mu) = 0.11 \quad (100)$$

$$\text{Br}(\tilde{\tau}_1 \rightarrow \mu^- \nu_\tau) = 0.10 \quad (101)$$

The stau now dominantly decays hadronically. In this specific case, we can have still a roughly 25% branching ratio to charged leptons. Or a probability of roughly 6% for two charged leptons in the final state. However, recall that we only scanned couplings down to  $10^{-7}$ . Thus we would expect solutions with even smaller  $\ell_{1,2}$ . In this case we would have purely hadronic final states and we must resort to the techniques used in Ref. [74], where the  $\bar{U}\bar{D}\bar{D}$  R-parity violating operators were studied.

## IX. CONCLUSIONS AND OUTLOOK

We have presented a simple ansatz for the  $B_3$  Yukawa couplings, relating them directly to the corresponding

Higgs Yukawa couplings via a small set of parameters  $\ell_i, \ell'_j$ . This results in simple relations between the  $B_3$  couplings presented in Tables I and II. We have given estimates of these parameters in order to obtain the correct neutrino masses and have then numerically determined the precise values. These are summarised in Tables III, IV. We then discussed the resulting collider signals for the case of a stau LSP. Depending on the fit values, we have found a wide range for the possible branching ratios of the stau-LSP. In forthcoming work, we shall give a detailed investigation of how to disentangle these models at the LHC.

## ACKNOWLEDGMENTS

We are grateful to Wilfried Buchmüller and Reinhold Ruckl for initiating the discussion on this ansatz and for providing us with their private notes. We thank Markus Bernhardt for valuable help and discussions on the  $B_3$  version of SOFTSUSY. We thank Christoph Luhn, Ulrich Langenfeld and Sebastian Grab for helpful discussions and Alejandro Ibarra and Laura Covi for valuable comments.

- 
- [1] B. T. Cleveland *et al.*, *Astrophys. J.* **496** (1998) 505; Y. Fukuda *et al.* *Phys. Rev. Lett.* **82** (1999) 2644 [arXiv: hep-ex/9812014]. Y. Fukuda *et al.* *Phys. Rev. Lett.* **81** (1998) 1158 [Erratum-ibid. **81** (1998) 4279] [arXiv: hep-ex/9805021]; W. Hampel *et al.* *Phys. Lett. B* **447** (1999) 127; J. N. Abdurashitov *et al.* *Phys. Rev. C* **60** (1999) 055801 [arXiv: astro-ph/9907113]; Q. R. Ahmad *et al.* *Phys. Rev. Lett.* **89** (2002) 011301 [arXiv: nucl-ex/0204008]; B. Aharmim *et al.* *Phys. Rev. C* **72** (2005) 055502 [arXiv:nucl-ex/0502021]; M. Apollonio *et al.* *Eur. Phys. J. C* **27** (2003) 331 [arXiv:hep-ex/0301017].
  - [2] L. Wolfenstein, *Phys. Rev. D* **17** (1978) 2369; S. P. Mikheev and A. Y. Smirnov, *Sov. J. Nucl. Phys.* **42** (1985) 913 [*Yad. Fiz.* **42** (1985) 1441].
  - [3] M. M. Guzzo, A. Masiero and S. T. Petcov, *Phys. Lett. B* **260** (1991) 154; E. Roulet, *Phys. Rev. D* **44** (1991) 935; V. D. Barger, R. J. N. Phillips and K. Whisnant, *Phys. Rev. D* **44** (1991) 1629; H. K. Dreiner and G. Moreau, *Phys. Rev. D* **67** (2003) 055005 [arXiv:hep-ph/0211354]; R. Adhikari, A. Sil and A. Raychaudhuri, *Eur. Phys. J. C* **25** (2002) 125 [arXiv:hep-ph/0105119].
  - [4] D. G. Michael *et al.* *Phys. Rev. Lett.* **97** (2006) 191801 [arXiv:hep-ex/0607088].
  - [5] See the talk by C. Walter at *The XXXIII International Conference on High Energy Physics, Moscow*, Russian Federation, July 26 - August 2, 2006.
  - [6] M. C. Gonzalez-Garcia, arXiv:hep-ph/0410030.
  - [7] M. C. Gonzalez-Garcia and M. Maltoni, arXiv: 0704.1800 [hep-ph].
  - [8] P. Minkowski, *Phys. Lett. B* **67** (1977) 421; T. Yanagida, *proc. of the Workshop: Baryon Number of the Universe and Unified Theories, Tsukuba, Japan, 1979*; M. Gell-Mann, P. Ramond, R. Slansky, in the *proc. of the Supergravity Stony Brook Workshop*, ed. by P. van Nieuwenhuizen & D.Z. Freedman (North Holland Publ. Co.), 1979; R. N. Mohapatra, G. Senjanovic, *Phys. Rev. Lett.* **44** (1980) 912.
  - [9] For reviews see: H. P. Nilles, *Phys. Rept.* **110** (1984); H. Haber, G. Kane, *Phys. Rept.* **117** (1985) 75; S. P. Martin, arXiv:hep-ph/9709356; M. Drees, R. Godbole, P. Roy, *Hackensack, USA: World Scientific (2004) 555 p*
  - [10] L. J. Hall, M. Suzuki, *Nucl. Phys. B* **231** (1984) 419.
  - [11] B. C. Allanach, A. Dedes and H. K. Dreiner, *Phys. Rev. D* **69** (2004) 115002 [Erratum-ibid. **D 72** (2005) 079902] [arXiv:hep-ph/0309196].
  - [12] H. K. Dreiner, C. Luhn and M. Thormeier, *Phys. Rev. D* **73** (2006) 075007 [arXiv:hep-ph/0512163].
  - [13] H. K. Dreiner, C. Luhn, H. Murayama and M. Thormeier, arXiv:0708.0989 [hep-ph].
  - [14] L. Ibañez and G. G. Ross, *Nucl. Phys. B* **368**, 3 (1992).
  - [15] H. K. Dreiner, arXiv:hep-ph/9707435.
  - [16] R. Barbier *et al.*, arXiv:hep-ph/0406039; G. Bhat-tacharyya, arXiv:hep-ph/9709395.
  - [17] M. Hirsch, M.A. Diaz, W. Porod, J.C. Romao, J.W.F. Valle, *Phys. Rev. D* **62** (2000) 113008 [Erratum-ibid. **D 65** (2002) 119901] [arXiv:hep-ph/0004115].
  - [18] M.A. Diaz, M. Hirsch, W. Porod, J. Romao, J. Valle, *Phys. Rev. D* **68** (2003) 013009



- [arXiv:hep-ph/0302021].
- [19] Y. Grossman and H. E. Haber, Phys. Rev. D **59**, 093008 (1999) [arXiv:hep-ph/9810536].
- [20] S. Davidson, M. Losada, Phys. Rev. D **65** (2002) 075025 [arXiv: hep-ph/0010325]; S. Davidson, M. Losada, JHEP **0005** (2000) 021 [arXiv: hep-ph/ 0005080].
- [21] R. Hempfling, Nucl. Phys. B **478** (1996) 3 [arXiv:hep-ph/9511288].
- [22] F. Borzumati, Y. Grossman, E. Nardi and Y. Nir, Phys. Lett. B **384** (1996) 123 [arXiv:hep-ph/9606251].
- [23] E. Nardi, Phys. Rev. D **55** (1997) 5772 [arXiv:hep-ph/9610540].
- [24] B. de Carlos and P. L. White, Phys. Rev. D **54** (1996) 3427 [arXiv:hep-ph/9602381].
- [25] V. D. Barger, M. S. Berger, R. J. Phillips and T. Wohrmann, Phys. Rev. D **53** (1996) 6407 [arXiv: hep-ph/9511473]; B. C. Allanach, A. Dedes and H. K. Dreiner, Phys. Rev. D **60** (1999) 056002 [arXiv:hep-ph/9902251]; H. K. Dreiner and H. Pois, arXiv:hep-ph/9511444.
- [26] A. H. Chamseddine, R. Arnowitt and P. Nath, Phys. Rev. Lett. **49** (1982) 970. S. K. Soni and H. A. Weldon, Phys. Lett. B **126** (1983) 215; L. J. Hall, J. D. Lykken and S. Weinberg, Phys. Rev. D **27** (1983) 2359.
- [27] C. Froggatt and H. B. Nielsen, Nucl. Phys. B **146**, 277 (1979).
- [28] H. K. Dreiner and M. Thormeier, Phys. Rev. D **69** (2004) 053002 [arXiv:hep-ph/0305270]. In this reference, we have summarized all existing Froggatt-Nielsen models which yield predictions for the proton hexality violating couplings.
- [29] See for example: H. K. Dreiner, C. Luhn, H. Murayama and M. Thormeier, Nucl. Phys. B **774** (2007) 127 [arXiv:hep-ph/0610026]. This paper summarizes all the Froggatt-Nielsen models to-that-date, which predict low-energy neutrino masses via baryon-triality couplings.
- [30] J. M. Mira, E. Nardi, D.A. Restrepo and J.W.F. Valle, Phys. Lett. B **492**, 81 (2000) [arXiv:hep-ph/0007266].
- [31] See for example: O. C. W. Kong, Mod. Phys. Lett. A **14** (1999) 903 [arXiv:hep-ph/9808304]; G. K. Leontaris, et al. Nucl. Phys. B **436** (1995) 461 [arXiv:hep-ph/9409369].
- [32] M. Drees, S. Pakvasa, X. Tata and T. ter Veldhuis, Phys. Rev. D **57** (1998) 5335 [arXiv:hep-ph/9712392].
- [33] E. J. Chun, S. K. Kang, C. W. Kim and U. W. Lee, Nucl. Phys. B **544** (1999) 89 [arXiv:hep-ph/9807327].
- [34] S. Y. Choi, E. J. Chun, S. K. Kang and J. S. Lee, Phys. Rev. D **60** (1999) 075002 [arXiv:hep-ph/9903465].
- [35] D. E. Kaplan and A. E. Nelson, JHEP **0001** (2000) 033 [arXiv:hep-ph/9901254].
- [36] A. Abada, S. Davidson and M. Losada, Phys. Rev. D **65** (2002) 075010 [arXiv:hep-ph/0111332].
- [37] B. Mukhopadhyaya, S. Roy and F. Vissani, Phys. Lett. B **443** (1998) 191 [arXiv:hep-ph/9808265].
- [38] A. Datta, B. Mukhopadhyaya and F. Vissani, Phys. Lett. B **492** (2000) 324 [arXiv:hep-ph/9910296].
- [39] W. Porod, M. Hirsch, J. Romao and J. Valle, Phys. Rev. D **63** (2001) 115004 [arXiv:hep-ph/0011248].
- [40] A. Datta, R. Gandhi, B. Mukhopadhyaya and P. Mehta, Phys. Rev. D **64** (2001) 015011 [arXiv:hep-ph/0011375].
- [41] E. J. Chun, D. W. Jung, S. K. Kang and J. D. Park, Phys. Rev. D **66** (2002) 073003 [arXiv:hep-ph/0206030].
- [42] V. D. Barger, T. Han, S. Hesselbach and D. Marfatia, Phys. Lett. B **538** (2002) 346 [arXiv:hep-ph/0108261].
- [43] M. Hirsch, W. Porod, J. C. Romao and J. Valle, Phys. Rev. D **66** (2002) 095006 [arXiv:hep-ph/0207334].
- [44] M. Hirsch, T. Kernreiter and W. Porod, JHEP **0301** (2003) 034 [arXiv:hep-ph/0211446].
- [45] M. B. Magro, F. de Campos, O. J. P. Eboli, W. Porod, D. Restrepo and J. W. F. Valle, JHEP **0309** (2003) 071 [arXiv:hep-ph/0304232].
- [46] M. Hirsch and W. Porod, Phys. Rev. D **68** (2003) 115007 [arXiv:hep-ph/0307364].
- [47] F. de Campos, O. J. P. Eboli, M. B. Magro, W. Porod, D. Restrepo and J. W. F. Valle, Phys. Rev. D **71** (2005) 075001 [arXiv:hep-ph/0501153].
- [48] S. P. Das, A. Datta and M. Guchait, Phys. Rev. D **70** (2004) 015009 [arXiv:hep-ph/0309168].
- [49] D. W. Jung, S. K. Kang, J. D. Park and E. J. Chun, JHEP **0408** (2004) 017 [arXiv:hep-ph/0407106].
- [50] A. Datta, J. Saha, A. Kundu and A. Samanta, Phys. Rev. D **72** (2005) 055007 [arXiv:hep-ph/0507311].
- [51] S. P. Das, A. Datta and S. Poddar, Phys. Rev. D **73** (2006) 075014 [arXiv:hep-ph/0509171].
- [52] A. Datta and S. Poddar, Phys. Rev. D **75** (2007) 075013 [arXiv:hep-ph/0611074].
- [53] S. Rakshit, G. Bhattacharyya and A. Raychaudhuri, Phys. Rev. D **59** (1999) 091701 [arXiv:hep-ph/9811500].
- [54] A. Abada and M. Losada, Nucl. Phys. B **585** (2000) 45 [arXiv:hep-ph/9908352].
- [55] A. Abada and M. Losada, Phys. Lett. B **492** (2000) 310 [arXiv:hep-ph/0007041].
- [56] A. Abada, G. Bhattacharyya and M. Losada, Phys. Rev. D **66** (2002) 071701 [arXiv:hep-ph/0208009].
- [57] See for example: J. Butterworth and H. Dreiner, Nucl. Phys. B **397** (1993) 3 [arXiv:hep-ph/9211204]; J. Erler, J. L. Feng and N. Polonsky, Phys. Rev. Lett. **78** (1997) 3063 [arXiv:hep-ph/9612397]; H. Dreiner, P. Richardson and M. H. Seymour, Phys. Rev. D **63** (2001) 055008 [arXiv:hep-ph/0007228]; H. Dreiner, S. Grab, M. Kramer and M. K. Trenkel, Phys. Rev. D **75** (2007) 035003 [arXiv:hep-ph/0611195].
- [58] B. C. Allanach, M. A. Bernhardt, H. K. Dreiner, C. H. Kom and P. Richardson, Phys. Rev. D **75** (2007) 035002 [arXiv:hep-ph/0609263].
- [59] S. Davidson, D. C. Bailey and B. A. Campbell, Z. Phys. C **61** (1994) 613 [arXiv:hep-ph/9309310].
- [60] A. Y. Smirnov and F. Vissani, Phys. Lett. B **380** (1996) 317 [arXiv:hep-ph/9601387].
- [61] B. C. Allanach, A. Dedes and H. K. Dreiner, Phys. Rev. D **60** (1999) 075014 [arXiv:hep-ph/9906209].
- [62] H. K. Dreiner, M. Kramer and B. O'Leary, Phys. Rev. D **75** (2007) 114016 [arXiv:hep-ph/0612278]; H. K. Dreiner, G. Polesello and M. Thormeier, Phys. Rev. D **65** (2002) 115006 [arXiv:hep-ph/0112228].
- [63] H. K. Dreiner and G. G. Ross, Nucl. Phys. B **365** (1991) 597.
- [64] K. Agashe and M. Graesser, Phys. Rev. D **54** (1996) 4445 [arXiv:hep-ph/9510439].
- [65] W. M. Yao *et al.* [Particle Data Group], J. Phys. G **33** (2006) 1.



- [66] Y. Grossman and S. Rakshit, Phys. Rev. D **69** (2004) 093002 [arXiv:hep-ph/0311310].
- [67] This rotation was first discussed in [10]. The most general case with complex parameters is given in [28].
- [68] See Fig. 9.2 and Eq. (9.17) in: R. N. Mohapatra and P. B. Pal, World Sci. Lect. Notes Phys. **60** (1998) 1 [World Sci. Lect. Notes Phys. **72** (2004) 1]. Note that there is a typo in the equation and the functions  $K$  should be replaced by  $K^2$ . (R.N. Mohapatra, *privat communication*).
- [69] A. Osipowicz *et al.* [KATRIN Collaboration], arXiv: hep-ex/0109033.
- [70] V. D. Barger, G. F. Giudice and T. Han, Phys. Rev. D **40** (1989) 2987.
- [71] H. Dreiner, Jong-Soo Kim, M. Thormeier, *Collider Signals of a Simple  $B_3$  Model for Neutrino Masses*. In preparation.
- [72] H. K. Dreiner, P. Richardson and M. H. Seymour, JHEP **0004** (2000) 008 [arXiv:hep-ph/9912407].
- [73] J. F. Gunion and H. E. Haber, Nucl. Phys. B **272** (1986) 1 [Erratum-ibid. B **402** (1993) 567].
- [74] See for example: H. Baer, C. Kao and X. Tata, Phys. Rev. D **51** (1995) 2180 [arXiv:hep-ph/9410283]; B. C. Allanach *et al.*, JHEP **0103** (2001) 048 [arXiv:hep-ph/0102173].